Scientia Iranica A (2019) 26(4), 2212–2228

Sharif University of Technology
Scientia Iranica
Transactions A: Civil Engineering
http://scientiairanica.sharif.edu

Invited Paper

Development of fragility curves for existing residential steel buildings with concentrically braced frames

A. Bakhshi* **and H. Soltanieh**

Development of Civil Engineering, Sharif University of Technology, Tehran, P.O. Box 11155-9313, Iran.

Received 23 February 2019; received in revised form 29 May 2019; accepted 7 July 2019

KEYWORDS
Analytical fragility curve;
Steel concentrically braced frames;
OpenSees;
FEMA 356;
FEMA P695;
Truncated *IDA*;
Maximum likelihood method.

Abstract. The objective of this study is to develop analytical fragility curves for an ensemble of existing 3- to 6-story residential steel buildings with concentrically braced frames in 2 directions, designed during 2010 to 2015 in Qazvin, Iran. The buildings were modeled three-dimensionally in OpenSees considering braces buckling behavior. Maximum Inter-story Drift Ratio ($MIDR$) and spectral acceleration at fundamental period of the structure with 5% viscous damping ($S_a(T_1, 5\%)$) were considered as Damage Index (DI) and Intensity Measure (IM), respectively. Limit states were specified as discussed in FEMA 356. Ground motion record selection and uncertainties assessment were carried out based on FEMA P695 methodology. Analysis was performed using truncated Incremental Dynamic Analysis (IDA). Fragility function was defined as a log-normal Cumulative Distribution Function (CDF) and maximum likelihood method was used to estimate fragility parameters. According to the fragility curves obtained, seismic vulnerability of the structures generally increased as the number of stories rose. Concentration of the inelasticity was also found to be mainly at the first story level. The results also confirmed the fact that the record to record variability is the main source of uncertainty in structural probabilistic evaluation.

1. Introduction

Seismic risk evaluation, vulnerability analysis, and loss estimation are considered as the first essential steps in sseismic hazard reduction of structures. Developing countries are typically more vulnerable to seismic hazard, such as earthquakes. Iran is also one of the developing countries prone to earthquakes. Qazvin, located north-west of the country and surrounded by several important faults, including Rudbar, Alamtrud, North Qazvin, Zanjan, Soltanieh, and Taleghan, is classified as a region with very high seismicity based on the *Iranian code of practice for seismic resistant design of buildings (Standard no. 2800)* [1]. Significant earthquakes (e.g., Buyin Zahra (1962) and Manjil (1990)) in the past with huge damages and losses are proofs of this issue. Thus, seismic vulnerability assessment of existing buildings in the city may be of great help.

Structural vulnerability to earthquake is usually expressed in terms of fragility curves or damage functions. Fragility curves represent the probability of the structural response exceeding a specific limit state at a given seismic intensity level. They can be constructed using several approaches including empirical, experimental, computational (analytical), and hybrid. Each of the abovementioned approaches have their own advantages and disadvantages. It should be noted that

*. *Corresponding author. Tel.: +98 21 66164243; Fax: +98 21 66014828*
E-mail address: bakhshi@sharif.edu (A. Bakhshi)

doi: 10.24200/sci.2019.21498

there is no universally accepted and best method of constructing fragility curves for all types of structures and, depending on the circumstances, one method should be applied [2].

Numerous studies have formerly been conducted concerning the development of fragility curves. In 2016, Kumar et al. [3] conducted Rapid Visual Screening (RVS) for 5 types of buildings in Himachal Pradesh State in India. RVS scores for 9099 buildings were calculated and the distribution of each building type was measured in this study. In 2017, fragility curves for RC buildings were proposed by Del Gaudio et al. [4] using a database of 7597 private buildings after the 2009 L'Aquila earthquake. The European Macro Seismic scale (EMS-98) was applied in order to measure damage grades. The proposed fragility curves were also compared with the main empirical fragility curves for RC buildings in the literature. In 2016, a study was carried out on the possible seismic damage to the residential buildings in Bucharest, Romania, by Toma-Danila and Armaş [5]. For this purpose, they used the improved displacement coefficient analytical method to compute damage probabilities based on 48 vulnerability curves for buildings included in the SELENA software. Deterministic seismic hazard scenarios were used in order to determine the intensity of the ground motion.

In Iran, the first study on fragility curves was conducted by Tavakoli and Tavakoli [6] in 1993 based on the data derived from Manjil-Rudbar earthquake in 1990. Some parameters such as construction year, seismic code, and height and type of structure were not included in this study. In 2000, vulnerability curves for 9 types of structures in Tehran were developed by the Japan International Cooperation Agency (JICA) [7] using the ATC-13 method, fragility curves developed by Tavakoli and Tavakoli [6], and engineering judgment. Mostafaei and Kabeyasawa [8] investigated the damage to buildings in the 2003 Bam earthquake. Bakhshi and Karimi [9] studied a method of developing fragility curves for seismic assessment of reinforced and unreinforced masonry buildings in Iran. For this purpose, the cumulative absolute velocity was considered as an *IM*.

In 2006, a *PGA*-based analytical fragility function was developed for masonry buildings in Tehran by Jalalian [10]. Kazemi et al [11] studied the impacts of various strong ground motion records on fragility curves for Mashhad city in Iran. In 2015, Sadeghi et al [12] conducted a study to derive the vulnerability curves for 42 types of Iranian buildings. For this purpose, logic-tree method was applied while considering the seismic code, construction provisions, and engineering judgment. In 2017, Kazemi et al. [13] determined fragility curves for steel braced frame structures using new spectral shape indicators and a weighted DI. They concluded that the spectral shape indicators strongly affected the predicted median structural capacities [13].

In 2018, Izanloo and Yahyaabadi [14] developed structural fragility curves for various building types based on realistic data obtained after the Sarpol-e Zahab earthquake in 2017. Two hundred buildings of various types were surveyed in different parts of the city in order to identify the real damage scenario. The HAZUS methodology was also used to determine the structural damage state of each building.

Table 1 presents a list of some fragility studies of steel structures. Although these studies may be effective in risk evaluation and mitigation program of a country, reviewing literature indicates that there are only few fragility studies focused on existing buildings, particularly in developing and earthquake-prone countries. The aim of this study is to assess seismic vulnerability through development of analytical fragility curves for a number of existing buildings in Qazvin. In order to obtain comprehensive and extensible results to the greatest extent, occupancy category, number of stories, and type of the structural system were selected such that the majority of the statistical population was covered. Therefore, building typology was carried out using the information obtained from both *Qazvin Statistics and IT Organization and Qazvin Construction Engineering Organization.* Based on the information obtained from *Qazvin Statistics and IT organization*, among a total of approximately 56000 buildings recorded, about 83% and 94.5% were steel and residential buildings, respectively. Furthermore, according to the information obtained from *Qazvin Construction Engineering Organization* (2010-2015), almost 98% of the recorded buildings had 3 to 6 stories. Only less than 2% of structures recorded within this period had less than 3 and more than 6 stories. It should also be noted that no information was recorded regarding the type of the seismic force resisting system.

Thus, in this study, 10 existing 3- to 6-story residential steel buildings with steel concentrically braced frames in both directions, designed during 2010 to 2015 according to *the Iranian code No. 6 for design loads for buildings* [15], *the Iranian Code No. 2800 for Seismic Restraint Design of Buildings (third edition)* [1], and *the Iranian code No. 10 for Design and Construction of Steel Structures* [16], were selected. The input available for each building was its structural model in ETABS [17]. The selected buildings were remodeled three-dimensionally in OpenSees [18]. Effort was made so that the actual behavior of structural systems under study and their failure modes were considered as far as possible. This included three-dimensional modeling, performing nonlinear dynamic analysis, and modeling buckling behavior of the braces using the method proposed by Uriz and Mahin [19]. Therefore, the results of this study would be of importance due to

Table 1. Review of some fragility studies conducted for steel structures in recent years.

Reference	Intensity Measure (*IM*)	Damage index (DM)	Comments
Kinali and Ellingwood (2007) [21]	S_a	Inter-story drift angle	• Fragility curves for 3-, 4- and 6-story steel frames designed to 1993 National Building Code, 1948 San Francisco Code and 1991 Standard Building Code respectively. • Three limit states considered (IO, SD (Structural Damage), CP).
Bermúdez et al. (2008) [22]	S_d	Yield and ultimate displacement	• Fragility curves for 4-story curved plan steel building designed to 1998 Columbian Code. • Capacity spectrum method used. HAZUS damage state definition used. Separate curves for each damage state for braced frame and for moment-resisting frames.
Kazantzi et al. (2008) [23]	S_a	Maximum inter-story drift	• Fragility curves derived for 5-story mid-rise steel frame designed to EC8 standard. • Time-history analysis undertaken using European records. • Two limit states considered (LS, CP), and curves defined for finite and unlimited joint ductility.
Li and Ellingwood (2008) [24]	S_a	Maximum inter-story drift ratio	• Fragility curves for 9- and 20-story steel moment resisting frame buildings - designed to 1994 UBC. • Three limit states considered (IO, LS, CP).
Ellingwood and Kinali (2009) [25]	S_a	Maximum inter-story drift angle	• Fragility analysis for 2- and 4-story partially restrained moment frames and a 6-story cross braced frame. • Fragility curves for three damage states (IO, LS, CP).
Majd et al. (2012) [26]	PGA	Inter-story drift and axial plastic deformation of bracing elements	• Fragility curves for 3-, 5- and 7-story steel buildings with X-bracing frames, regular in both plan and elevation. • Three limit states considered (IO, LS, CP).
Akbari et al. (2014) [27]	PGA	Critical inter-story drift	• Fragility curves for steel X-braced and chevron-braced RC frames. • HAZUS damage states (slight, moderate, extensive and Complete).
Kiani et al. (2016) [28]	S_a	Maximum inter-story drift	• Fragility curves for 3- and 5-story building models consisting of unbraced frames with masonry infill walls, braced frames with concentric bracings and braced frames with masonry infill walls. • ATC-63 procedures and methodologies. • Three limit states considered (IO, LS, CP).
Banihashemi et al. (2016) [29]	PGA	Maximum inter-story drift	• Four six- and nine-story chevron-type SCBFs designed as special steel concentrically braced frames, SCBFs, according to BHRC (2005) design spectra and AISC seismic provisions. • A newly developed performance-based plastic design (PBPD) methodology applied to SCBFs. • Two performance limit states considered (IO, CP).

Table 1. Review of some fragility studies conducted for steel structures in recent years (continued).

Reference	Intensity Measure (*IM*)	Damage index (DM)	Comments
Li et al. (2017) [30]	S_a	The frame ductility normalized with respect to the frame yield displacement	• Low-ductility steel concentrically braced frame modeled as a SDOF system. • The Incremental Dynamic Analysis (*IDA*) adopted to construct the collapse ductility spectrum.
Choi et al. (2017) [31]	S_a	Maximum inter-story drift ratio	• Nonlinear static and dynamic analyses of 5- and 10-story steel ordinary concentrically braced frames (OCBFs). • Evaluating collapse capacities using collapse probabilities evaluation method described in FEMA P695. • Three damage states considered (elastic, yielding, failure).
Díaz et al. (2018) [32]	Spectral displacement	Park and Ang damage index	• Three steel buildings namely high- (13 stories), mid- (7 stories) and low-rise (3 stories) buildings, with Special Moment Frames (SMF).
Fattahi and Gholizadeh (2019) [33]	S_a	Maximum inter-story drift ratio	• Seismic performance assessment of optimally designed steel moment frames (SMFs). • Three numerical examples of 3-, 6-, and 12-story SMFs.

applying actual statistics recorded by the provincial organizations as well as accurate modeling of the existing buildings [20].

2. Seismic parameters and record selection

2.1. Seismic Damage Indices (DIs)

Quantification of damages to a structure during its service life has utmost importance. Seismic DIs are widely used for anticipating possible damages. They are formulated using response parameters of the structure obtained from structural analysis [34]. DIs may be classified in several various ways. If the criterion is the location of the damage occurrence, they would be classified into local or global DIs. Local DIs include deformation-based non-cumulative indices, energy-based cumulative indices, and combined indices. They may also be categorized as structural or non-structural, elastic or inelastic, and static or dynamic indices [35].

In this study, $MIDR$ is considered as the DI. It is a non-cumulative local index that has formerly been applied in several studies.

2.2. Seismic Intensity Measures (IMs)

An essential step in seismic vulnerability analysis and fragility curve construction is to select an appropriate earthquake IM that characterizes the strong ground motion and has the best correlation with the structural response of each element. Ground motion characteristics that influence the seismic performance of structures include intensity, frequency content, and duration of strong ground motions. IMs may be classified as qualitative and quantitative measures. The latter can be divided into peak-value-based energy and spectral parameters. Optimality of IMs can be defined in terms of practicality, effectiveness, efficiency, sufficiency, robustness, and computability [36].

A spectral IM that has been adopted in many studies so far is spectral acceleration at fundamental period of the structure with 5% viscous damping ($S_a(T_1, 5\%)$). Several studies have indicated that $S_a(T_1, 5\%)$ is more efficient than Peak Ground Acceleration (PGA) when the drift response is considered as the damage measure. As Mackie and Stojadinović [37] state, efficiency refers to the total variability of an Engineering Demand Parameter (EDP) for a given IM. In other words, variability of the damage measure is reduced at a specific IM value by selecting an efficient IM. Thus, lower number of nonlinear dynamic analyses and ground motion records is required in order to achieve accurate responses. Furthermore, since the analytical models used in this study have less than 8 stories, that is, they are not of structures with long periods and ground motion records used in the analyses are not of near-field type, the adopted IM ($S_a(T_1, 5\%)$) is efficient and effective. This was also verified by the study conducted in 2013 by Fathieh [38].

Table 2. Summary of the earthquake event data for the far-field record set used in this study [39].

Record no.	Earthquake			NEHRP class	Source (fault type)	Recorded motions	
	M	Year	Name			$PGA_{\max}$ (cm/s^2)	$PGV_{\max}$ (cm/s^2)
1	6.7	1994	Northridge	D	Thrust	0.52	63
2	6.7	1994	Northridge	D	Thrust	0.48	45
3	7.1	1999	Duzce, Turky	D	Strike-slip	0.82	62
4	7.1	1999	Hector Mine	C	Strike-slip	0.34	42
5	6.5	1979	Imperial Valley	D	Strike-slip	0.35	33
6	6.5	1979	Imperial Valley	D	Strike-slip	0.38	42
7	6.9	1995	Kobe, Japan	C	Strike-slip	0.51	37
8	6.9	1995	Kobe, Japan	D	Strike-slip	0.24	38
9	7.5	1999	Kocaeli, Turky	D	Strike-slip	0.36	59
10	7.5	1999	Kocaeli, Turky	C	Strike-slip	0.22	40
11	7.3	1992	Landers	D	Strike-slip	0.24	52
12	7.3	1992	Landers	D	Strike-slip	0.42	42
13	6.9	1989	Loma Prieta	D	Strike-slip	0.53	35
14	6.9	1989	Loma Prieta	D	Strike-slip	0.56	45
15	7.4	1990	Manjil, Iran	C	Strike-slip	0.51	65
16	6.5	1987	Superstition Hills	D	Strike-slip	0.36	46
17	6.5	1987	Superstition Hills	D	Strike-slip	0.45	36
18	7	1992	Cape Mendocino	D	Thrust	0.55	44
19	7.6	1999	Chi-Chi Taiwan	D	Thrust	0.44	115
20	7.6	1999	Chi-Chi Taiwan	C	Thrust	0.51	39
21	6.6	1971	San Fernando	D	Thrust	0.21	19
22	6.5	1976	Friuli, Italy	C	Thrust	0.35	31

2.3. Ground motion record selection

One of the main issues in dynamic structural analysis is the selection of ground motion records as well as their number so as to obtain results with desirable accuracy. The far-field record set suggested by FEMA P695 [39], which includes 22 pairs of records (44 individual components) selected from the PEER NGA database [40], is used in this study. There are several different criteria for selecting records in FEMA P695, which include source magnitude, source type, site conditions, site-source, number of records per event, strongest ground motion records, strong-motion instrument capability, and strong-motion instrument location.

Tables A-4A, A-4B, and A-4C of FEMA P695 present a summary of the magnitude, year, and the name of the event as well as the name and owner of the station; a summary of the site and source characteristics, epicentral distances, and various other measures of site-source distance; and a summary of key record information from the PEER NGA database [40], respectively [39]. Table 2 shows a list of the most important information associated with the record set used in this study.

3. Uncertainties

Uncertainties due to ground motion and structural properties are the main typical sources of uncertainty in earthquake engineering. The most significant sources of uncertainty in ground motion include those related to IM, Ground Motion Profile (GMP), and ground motion record selection. On the other hand, uncertainties in mass, viscous damping, strength, stiffness, structural geometry, and soil-structure interface are the main sources of uncertainty in structural properties. However, the former is known to be more difficult to characterize. Furthermore, several studies have indicated that uncertainties due to ground motion and record to record variability are significantly more important in vulnerability assessment of structures. These uncertainties are also found to be more considerable for global EDPs, namely $MIDR$, than for structural properties [41]. Thus, ignoring the variability due to material properties and considering uncertainty by applying a constant value at the end of the analyses seem to be acceptable in this study. This is in fact approved by the results of several studies that have

defined random nature of earthquake as the most important source of uncertainty in the probabilistic assessment of structures.

As discussed earlier, uncertainties due to variability of structural properties are not accounted for in this study. However, since they may be effective (although insignificantly) in deriving actual results, they can be expressed as quantitative values. Therefore, FEMA P695 [39] approach, which has been adopted in several previous studies, is applied herein for uncertainty calculations. In 2010, a trial application of this methodology was presented by Koutromanos and Shing [42], in which the collapse performance was evaluated for ordinary and special load bearing reinforced masonry shear wall systems designed according to the code provisions of the time. In 2011, a report was published by Donovan and Memari [43], which presented the results of a pilot project on the quantification of seismic performance factors for Structural Insulated Panels (SIPs) as the seismic force resisting system in residential and light commercial buildings based on the methodology presented in FEMA P695. In 2014, Pragalath & Sarkar [44] investigated the effect of the mentioned methodology on the seismic fragility evaluation of RC buildings and made comparisons with another conventional approach, which was based on a series of time history analyses and a power law representing probabilistic seismic demand model. In 2015, this method was adopted by Siyam [45], in which the seismic performance of 6 concrete block structural walls was investigated in order to evaluate their force-, displacement-, and performance-based seismic design parameters. Eventually, in 2016, Kiani [28] developed fragility curves for 3- and 5-story building models consisting of unbraced frames with masonry infill walls, braced frames with concentric bracings, and braced frames with masonry infill walls using this methodology.

In the FEMA P695 methodology, uncertainty index for record to record variability β_{RTR}, which is calculated by *IDA* analysis under different earthquake records, is added to quality rating for design requirements, test data, and index archetype models, which are introduced in Tables 3-1, 3-2 and 5-3 of FMA P695 [39] and shown as β_{DR}, β_{TD}, and β_{MDL}, respectively. They are associated with the uncertainty, which is factored into the performance evaluation of a proposed seismic force-resisting system.

Selecting the former implies completeness and robustness of the design requirements, and confidence in the basis for the design equations. Quantitative values for collapse uncertainty in relation to the design requirements are: (A) Superior, $\beta_{DR} = 0.10$; (B) Good, $\beta_{DR} = 0.20$; (C) Fair, $\beta_{DR} = 0.35$; and (D) Poor, $\beta_{DR} = 0.50$.

Selecting a quality rating for test data implies completeness and robustness of the overall testing program, and confidence in the test results. Quantitative values for this case include: (A) Superior, $\beta_{TD} = 0.10$; (B) Good, $\beta_{TD} = 0.20$; (C) Fair, $\beta_{TD} = 0.35$; and (D) Poor, $\beta_{TD} = 0.50$.

Finally, the lattermost is a combined assessment of:

1. How well index archetype models represent the range of structural collapse characteristics and the design parameters associated with the archetype design space; and
2. How well the analysis models capture structural collapse behavior through both direct simulation and non-simulated limit state checks.

The quantitative values of modeling-related collapse uncertainty are: (A) Superior, $\beta_{MDL} = 0.10$; (B) Good, $\beta_{MDL} = 0.20$; (C) Fair, $\beta_{MDL} = 0.35$; and (D) Poor, $\beta_{MDL} = 0.50$ [39].

According to the above discussions and the assumptions applied in this study, the corresponding values of β_{DR}, β_{TD}, and β_{MDL} are taken as 0.35, 0.35, and 0.2, respectively. Assuming all the indices are independent of each other, the total uncertainty index, β_{TOT}, is calculated from the square root of the sum of their squares as follows (Eq. (1)):

$$\beta_{TOT} = \sqrt{\beta_{RTR}^2 + \beta_{DR}^2 + \beta_{TD}^2 + \beta_{MDL}^2}. \quad (1)$$

4. Structural modeling

Concentrically braced frames are among the most widely used seismic force resisting systems in steel structures. These frames experience a wide range of Performance Levels (PLs) and can effectively sustain lateral drifts during frequent and moderate earthquakes through providing adequate lateral stiffness and strength. However, the bracing members may be subjected to large axial deformations during severe earthquakes, which in turn lead to large overall and local buckling deformations as well as tensile yielding. This inelastic response enables the braced frame to resist large cyclic drift demands. Eventually, one of the components will fail. Experimental studies show that the local buckling deformation, especially at the center of the brace, will finally result in tearing of the brace [46].

In this study, 10 existing residential steel structures designed during 2010 to 2015 with 3 to 6 stories and steel concentrically braced frames as the seismic force-resisting system in two directions are modeled three-dimensionally in OpenSees [18]. Several classification parameters including number of stories (n), number of braced frames in global X-Z ($nbXZ$) and Y-Z directions ($nbYZ$), and bracing configuration type

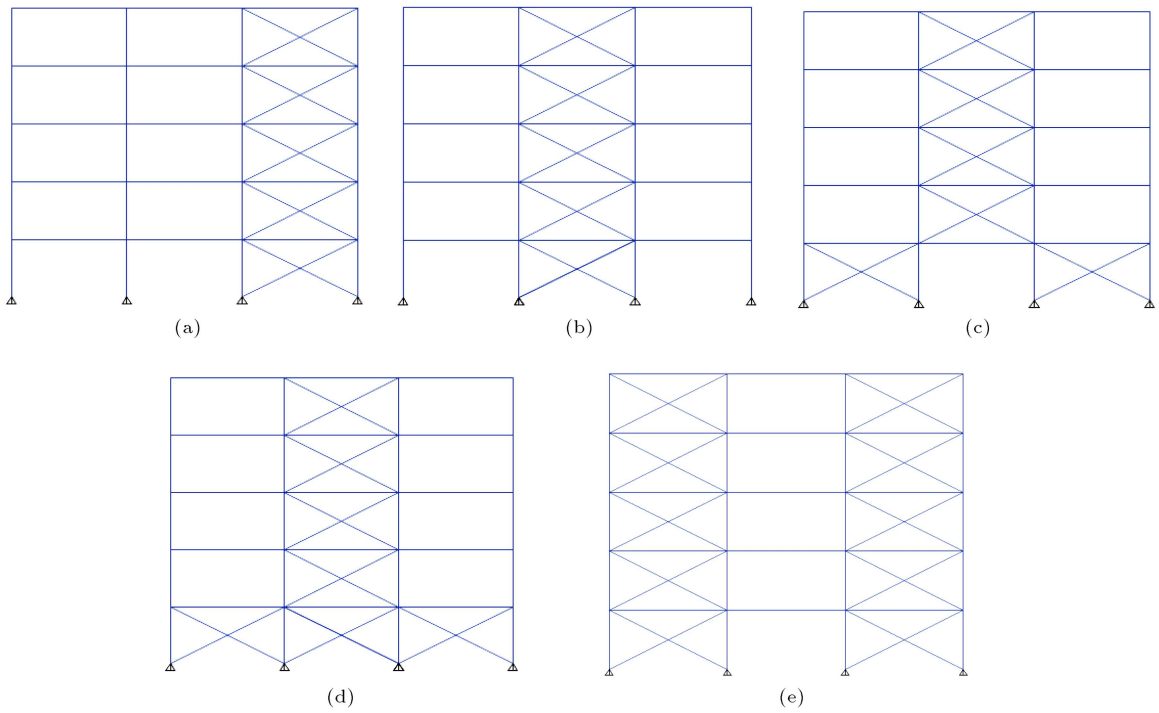

Figure 1. Typical bracing configuration types classified in this study.

($conf$) are considered to define the models. Five different configuration types are identified in the selected buildings, which are classified into "a" to "e". These configuration types are illustrated in Figure 1. In general, each model is expressed as $Mn - Ss - nbXZconf - nbYZconf$.

Material. Steel01 material object in OpenSees [18] is used to model steel with the strain-hardening ratio of $b = 0.02$. This type of material is used to construct a uniaxial bilinear steel material object with kinematic hardening and optional isotropic hardening described by a non-linear evolution equation [47]. Steel yield strength, F_y, and modulus of elasticity, E, are defined for each model based on the input information of the model. It should also be noted that this type of material is not able to model the brace over-strength in compression. The reason for this is the inability of this object to define different yield stresses in tension and compression.

Section. In order to build a section through the force-deformation response due to stress at the cross section of a beam-column element, fiber section object is used. Fiber section is discretized into smaller regions called patches in which the material stress-strain response is integrated to give the resultant behavior [47].

Element. To construct beam, column, and brace elements, nonlinear beam-column element object with 4 to 6 integration points along the length of the element is used, which is based on the non-iterative (or iterative) force formulation and considers the spread of plasticity along the element. The integration along the element is based on Gauss-Lobatto quadrature rule with two integration points at the ends of the element [47]. Furthermore, to represent the simple beam-to-column connections (pinned connections) and brace connection to beam-column joint, zero-length elements (rotational springs) are used, which are defined by two nodes at the same location. The nodes are connected by multiple material objects to represent the force-deformation relationship for the element. Two rotational springs are needed at both ends of the element with pinned connections. These springs are employed such that they can properly represent the pinned connection behavior. For this purpose, two elastic material objects, one with very large and another with very low axial stiffness, are primarily defined. In both springs, the elastic material object with very large axial stiffness, as defined earlier, is used in the direction corresponding to the bending in both axes. In order to avoid torsion around the element and the resulting instability, the abovementioned material with very large axial stiffness is employed in the local axis corresponding to torsion in only one of the springs located at the ends of the element.

Brace. Since the available element objects in OpenSees [18] are not capable of simulating buckling behavior in the brace elements, the model presented by Uriz and Mahin [19] is implemented. In the proposed approach, the brace element should be subdivided into

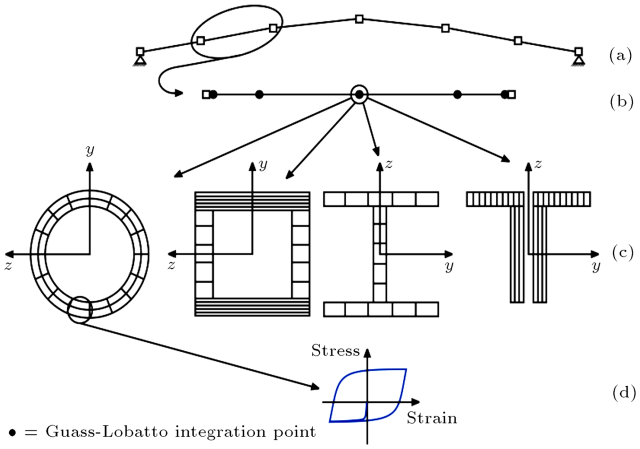

Figure 2. Schematic illustration of the proposed multi-element beam-column showing (a) initial camber-exaggerated, (b) monitored integration points, (c) ability to model multiple cross sections, and (d) uniaxial material model [19].

at least two elements. However, to accurately address local deformations and especially steel strains on the brace element, a better subdivision is required. A schematic representation of this model is presented in Figure 2.

In this study, each brace element is subdivided into 4 nonlinear beam-column elements. Therefore, 5 nodes (2 at both ends and 3 along interior parts of the element) should be defined. To model the buckling behavior, the node exactly at the middle of the brace element is subjected to out-of-plane imperfection equal to 0.1% its length. Thus, a quadratic perturbation shape is used to define the initial camber. Buckling behavior of brace elements is modeled using this approach in addition to the corotational geometric transformation.

Floor. RigidDiaphragm command is used in order to consider rigidity of the floors.

Geometric transformation. To transform beam element stiffness and resisting force from the basic system to the global-coordinate system, the geometric-transformation command (geomTransf) is used [47]. In this study, linear and P-Delta transformations to account for P-Delta effects are employed for beam and column elements, respectively. Corotational geometric transformation is used for brace elements, which enables us to consider large deformations such as those due to buckling of the brace elements.

Analysis parameters. Newmark integration method with $\beta = 0.25$ and $\gamma = 0.25$ is applied. Rayleigh damping equal to 5% is used for all elements except the rotational springs located at connections. It should also be noted that Krylov-Newton algorithm has primarily been applied. However, using one specific algorithm would not individually lead to convergence in most cases. Thus, it may be required to use a loop in the analysis and employ different algorithms and parameters in order to achieve convergence.

5. Nonlinear dynamic analysis, limit states, and fragility function

5.1. Incremental Dynamic Analysis (IDA)

One of the main issues in performance-based earthquake engineering is to evaluate the structural performance under seismic loads. In this context, an appropriate approach would be the use of IDA method. This includes performing nonlinear dynamic analyses of a structural model under a set of ground motion records, each scaled to multiple intensity levels and applied to the structural model such that they force the model through the entire range of behavior, from elastic to inelastic and finally to Global Instability (GI) [48].

When using this method, some records may require to be scaled to large IM levels in order to cause collapse. This may raise several concerns. First, it is computationally expensive to perform many structural analyses with increasing IM values in order to finally observe a collapse. Second, since the fragility function values at large intensity levels are of less interest than those at small IM levels, the results of large-IM levels are less practically relevant. Finally, it may be controversial whether scaling typical moderate IM ground motion records up to extreme IM levels is an accurate way to represent real seismic events of such large IM levels.

One possible strategy to address these concerns is performing truncated IDA by continuing the IDA only up to some level, namely $IM_{\max}$, above which no further analyses are performed. Thus, considering a total number of records used for performing truncated IDA, there will in general be m ground motion records, which cause collapse at IM levels lower than $IM_{\max}$, and $n - m$ ground motions that do not cause collapse prior to the analyses being stopped [49].

In this study, truncated IDA with $IM_{\max} = 2.0$ g and an intensity increment equal to 0.2 g is used to analyze the structural models. In this regard, first, acceleration spectrum is obtained for all ground motion records; then, the set of records is scaled to the spectral acceleration corresponding to the fundamental period of the structure. The scaling procedure and dynamic analysis are continued until the spectral acceleration corresponding to the fundamental period of the structure reaches 0.2 g ($IM_{\max}$). In this study, a total of 2200 nonlinear time history analyses (10 models, 22 records, 10 intensity levels) are performed for constructing fragility curves.

Table 3. Structural (Performance Levels) PLs and damage to braced steel frames in FEMA 356 [50].

Elements	Type	Structural performance levels		
		Collapse Prevention (CP)	**Life Safety (LS)**	**Immediate Occupancy (IO)**
Braced steel frames	Primary	Extensive yielding and buckling of braces. Many braces and their connections may fail.	Many braces yield or buckle but do not totally fail. Many connections may fail.	Minor yielding or buckling of braces.
	Secondary	Same as primary	Same as primary	Same as primary
	Drift	2% transient or permanent	1.5% transient; 0.5% permanent	0.5% transient; negligible permanent

5.2. Damage states and Performance Levels (PLs)

As noted earlier, $MIDR$ is considered as DI in this study. Quantification of the relationship between DI, which quantifies the damage using analytical models, and the damage states, which provide categorization of the observed seismic damage, is of great importance in fragility curve construction. The overall damage to an ordinary building can be classified as minor, moderate, or extensive, which is typically referred to as PL of that building under a given earthquake. These PLs, called "Immediate Occupancy" (IO), "Life Safety" (LS), and "Collapse Prevention" (CP) in FEMA 356 [33], are used in this study. For this purpose, the values given in Table C1-3 of FEMA 356 have been employed for interstory drifts (Table 3). Exceeding the value corresponding to each of the PLs by the selected DI is representative of fragility of the system under that specific PL [26].

5.3. Fragility function

To define a fragility function, a log-normal CDF is typically used (Eq. (2)). This implies that the IM values of ground motions causing collapse of a given structure are lognormally distributed.

$$P(C|IM = x) = \Phi\left(\frac{\ln(x/\theta)}{\beta}\right), \tag{2}$$

where, $P(C|IM = x)$ is the probability that a ground motion with $IM = x$ will cause the structure to collapse, $\Phi()$ is the standard normal CDF, θ is the median of the fragility function (the IM level with 50% probability of collapse), and β is the standard deviation of $\ln IM$ (sometimes referred to as the dispersion of IM). To calibrate Eq. (2) for a given structure, θ and β require to be estimated from structural analysis results.

5.3.1. Fragility parameters estimation using maximum likelihood method

The maximum likelihood method is employed to compute the likelihood of observing the data presented before, given a candidate fragility function. Using truncated IDA, IM values at collapse for the m ground motions that were observed to cause collapse (IM_i) are known. The likelihood that an arbitrary ground motion causes collapse at IM_i, given a fragility function defined by Eq. (2), is the normal distribution Probability Density Function (PDF) (Eq. (3)):

$$\text{Likelihood} = \phi\left(\frac{\ln(IM_i/\theta)}{\beta}\right). \tag{3}$$

In the above equation, $\phi()$ is the standard normal PDF. The $n - m$ ground motions that do not cause collapse up to $IM_{\max}$ are called censored data, since we only know that IM_i is greater than $IM_{\max}$. The likelihood that a given ground motion can be scaled to $IM_{\max}$ without causing collapse is equal to the probability that IM_i would be greater than $IM_{\max}$ (Eq. (4)):

$$\text{Likelihood} = 1 - \phi\left(\frac{\ln\left(IM_{\max}/\theta\right)}{\beta}\right). \tag{4}$$

Assuming that the IM_i values for each ground motion are independent, the likelihood of observing the entire dataset is the product (multiply) of the individual likelihoods (Eq. (5)):

$$\text{Likelihood} = \left(\prod_{i=1}^{m} \phi\left(\frac{\ln(IM_i/\theta)}{\beta}\right)\right) \left(1 - \phi\left(\frac{\ln(IM_{\max}/\theta)}{\beta}\right)\right)^{n-m}, \tag{5}$$

where Π is a product over i values from 1 to m (corresponding to the m ground motions that cause collapse at IM levels lower than $IM_{\max}$). To obtain fragility function parameters, they are varied such that the likelihood function is maximized. It is mathematically equivalent to and numerically easier by maximizing the logarithm of the likelihood function. Thus, in general, Eq. (6) holds [49]:

$$\{\theta, \beta\} = \arg\max_{\theta,\beta} \sum_{j=1}^{m} \left\{ \ln \phi \left(\frac{\ln(IM_i/\theta)}{\beta} \right) \right\} + (n-m) \ln \left(1 - \phi \left(\frac{\ln(IM_{\max}/\theta)}{\beta} \right) \right). \quad (6)$$

It is a maximization problem solved by MATLAB program [51] in this study.

6. Results and discussion

6.1. IDA curves

To develop fragility curves, truncated IDA under the FEMA P695 far-field record set is performed for each model using OpenSees [18]. IDA curves for $M6-S5-2BB-2CC$, which is a 5-story steel building with 2 concentrically braced frames of configuration type "B" and "C" (see Figure 1) in each direction, respectively, are plotted in Figure 3, as an example. From this figure, one can observe that IDA curves are quite record-sensitive. In fact, various dissimilar IDA curves are produced for a given structure under different ground motion records. However, a distinct elastic linear region ranging up to about 0.4 g is recognizable in almost all curves. This IM value corresponds to the first brace buckling occurrence. The slope of this elastic region, called elastic stiffness, may vary to some extent from record to record. With the first element in the system exhibiting nonlinear behavior, the elastic region ends.

IDA curves under 4 records of the record set are presented in Figure 4 in order to more clearly illustrate the different behaviors shown by these curves, including gradual degradation toward rapid instability to oscillating non-monotonic wavy behavior. From Figure 4(a)-(d), it can be seen that there are considerable differences in the shapes of the IDA curves and consequently, in what they refer to. Given the case in Figure 4(a), it can be seen that the IDA curve rapidly softens after the occurrence of the first buckling through shifting toward larger drifts and eventually, instability. In Figure 4(b), a slight hardening can be observed. On the other hand, Figure 4(c) indicates severe hardening at several IM values by great local increase in stiffness compared to the previous case. Wavy behavior due to hardening can also be observed in Figure 4(d). Thus, it can be seen that in some regions, despite the rise in IM values, the DI has decreased and as a result, the IDA curve is shifted backward to relatively lower drifts, making it a non-monotonic function of the IM. In fact, as the IM values increase, the inconsiderable, non-effective response at outset of the time-history becomes stronger and can lead to earlier damage or yielding development in the structure. This may alter the initial properties of the structure and consequently, affect the subsequent, more considerable response. The hardening behavior in IDA curve can also be found in Figure 5.

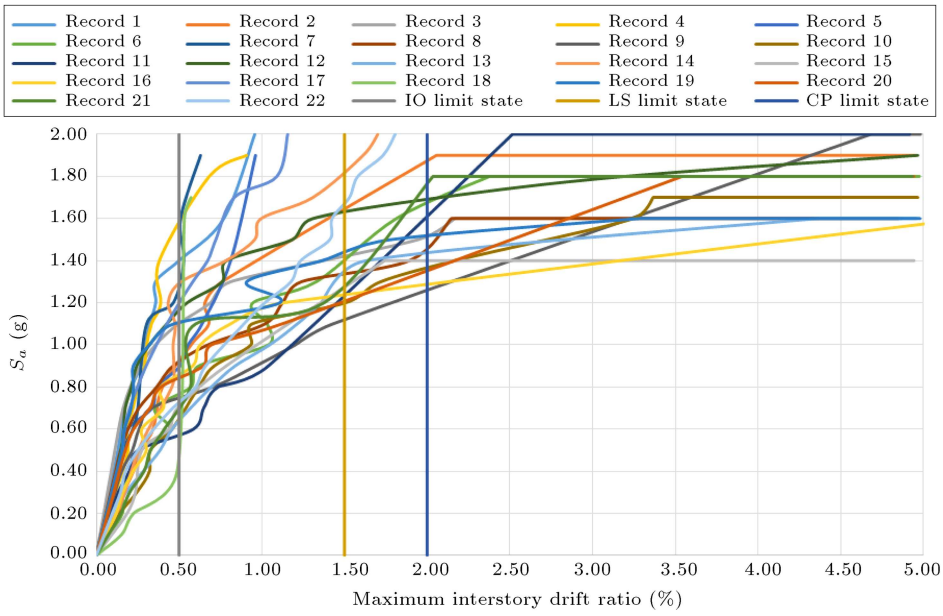

Figure 3. IDA curves for $M6-S5-2BB-2CC$ under the FEMA p695 far-field record set.

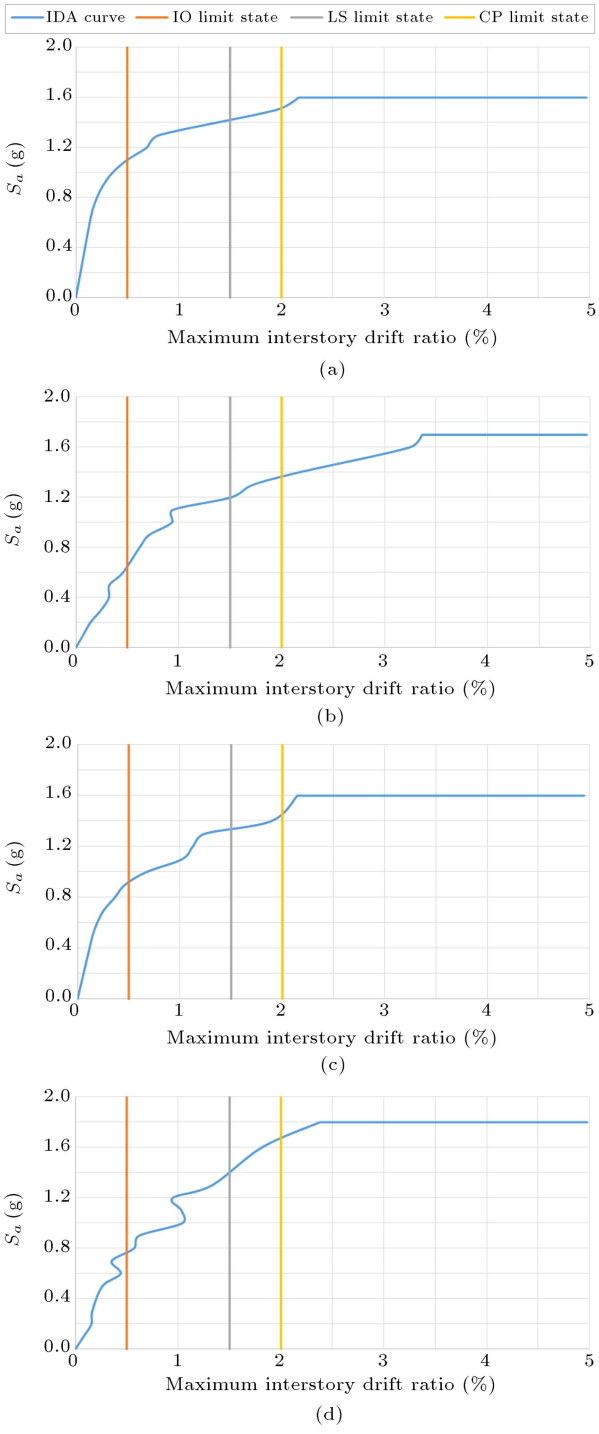

Figure 4. IDA curves for $M6 - S5 - 2BB - 2CC$ under 4 records of the FEMA p695 far-field record set, showing different behaviors: (a) Rapidly softening after the first buckling, (b) slight hardening, (c) severe hardening, and (d) wavy behavior.

Another behavior shown by IDA curve is illustrated in Figure 6. In this case, the analysis may stop due to convergence problems at a given IM value. However, it may exhibit stability under the next higher IM value. The phenomenon in which the structure

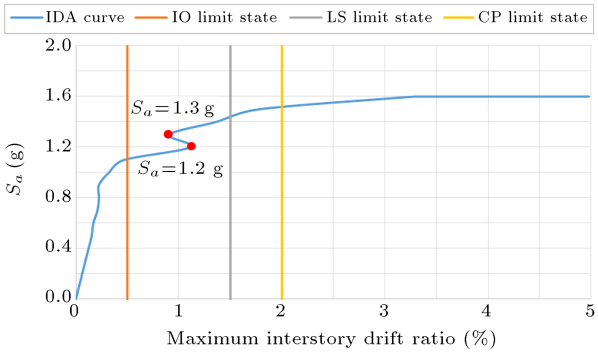

Figure 5. An example of hardening behavior in IDA curve for $M6 - S5 - 2BB - 2CC$.

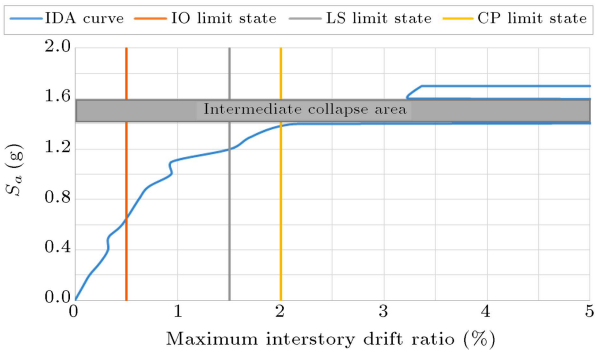

Figure 6. Single IDA curve for $M5 - S5 - 2BB - 2CC$ showing "structural resurrection".

remains stable after it experiences collapse in the previous cycles is known as "Structural Resurrection" [52]. The cycle(s) in which non-convergence happens are shown as intermediate collapse areas, which are located between two stable analysis cycles.

6.2. Fragility curves

Fragility curves for the structural models are developed and plotted in Figures 7 and 8. The probability of exceeding each limit state at any given IM value can be obtained using these curves. As can be seen, the fragility curves are derived taking into account 2 situations by considering the uncertainty due to record to record variability, β_{RTR}, (the upper curve), which is obtained directly from the IDA results, and the total uncertainty index, β_{TOT} (the lower curve), which is associated with quality rating for the design requirements, test data, and index archetype. It can be observed that the fragility curves in the latter case have a wider and flatter form and thus, lower values of the probability of exceeding a limit state at a specific IM value than those in the former case. This is due to increase in uncertainties and consequently, in the value of β in the fragility function. This confirms the fact that the record to record variability is the main source of uncertainty in the probabilistic evaluation of the structures and thus, considering it individually is

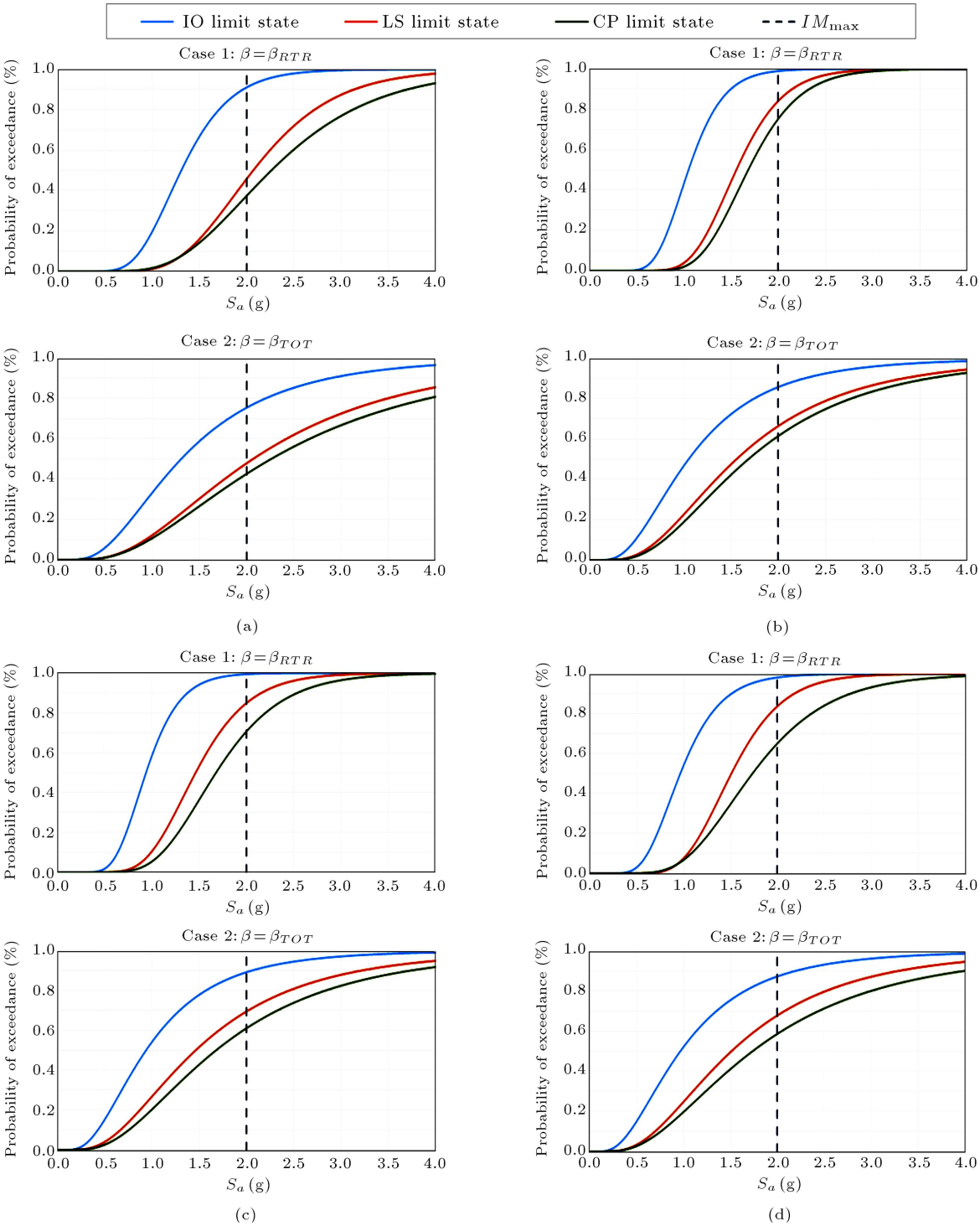

Figure 7. The obtained fragility curves for 3- and 4-story models: (a) $M1-S3-1A-2EE$, (b) $M2-S3-2AA-2BB$, (c) $M3-S4-1A-2BB$, and (d) $M4-S4-1A-1A$.

a conservative approach. Figures 7 and 8 also indicate that the fragility curves associated with LS and CP limit states are quite close to each other for almost all models. This may be due to the insignificant differences between the threshold values corresponding to the PLs in FEMA 356 [50].

6.3. Sensitivity analysis

Fragility curves for 4 sets of models (each set corresponding to one specific story number) are plotted in Figure 9. It is obvious from this figure that, in general, the fragility curve is pulled back to lower intensity levels as the number of stories increases. This suggests that

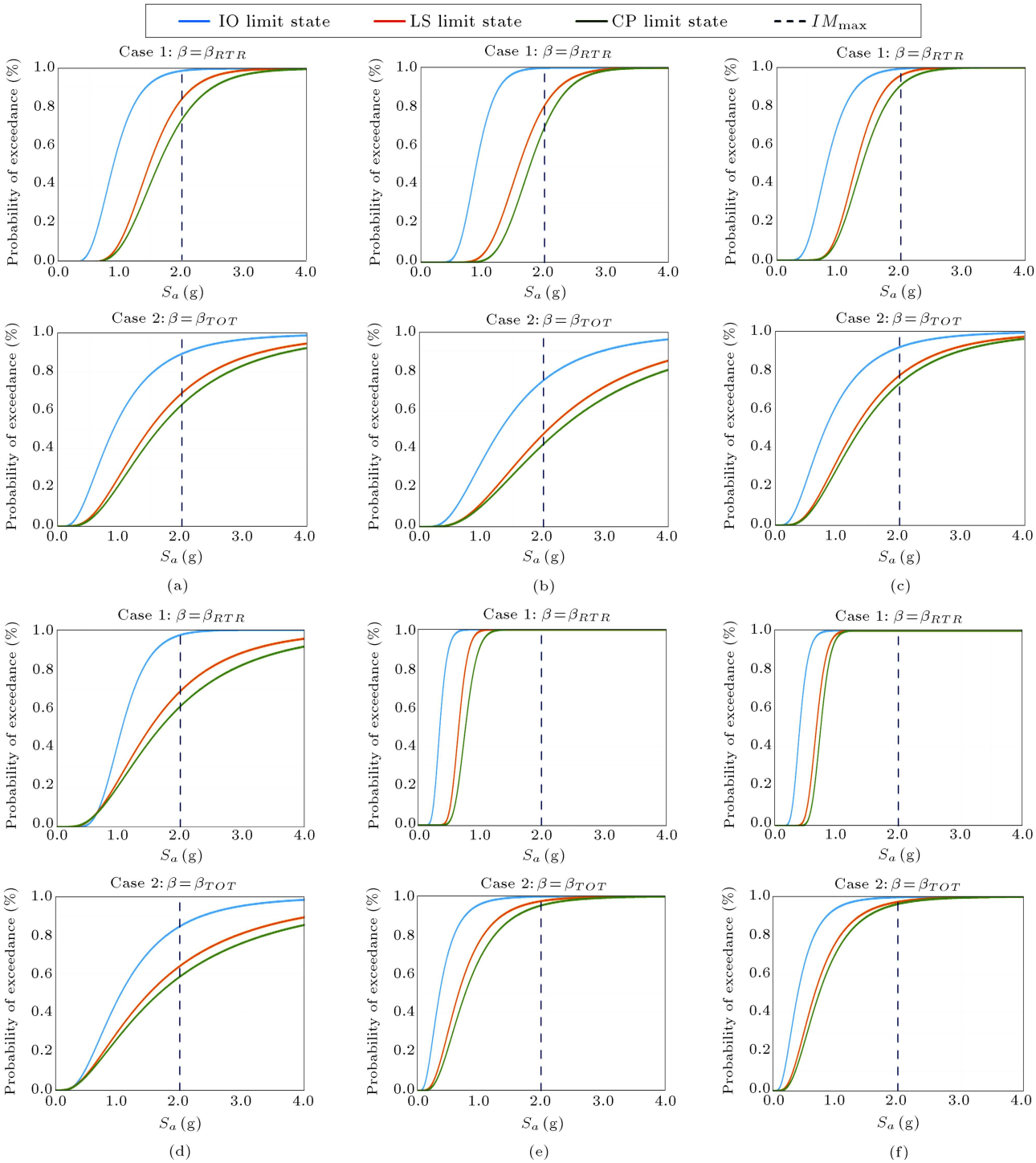

Figure 8. The obtained fragility curves for 5- and 6-story models: (a) $M5-S4-2AA-2AA$, (b) $M6-S5-2BB-2CC$, (c) $M7-S5-2AA-2AA$, (d) $M8-S5-2BB-2BB$, (e) $M9-S6-2AA-2CC$, and (f) $M10-S6-2AA-2DD$.

seismic vulnerability generally increases with the rise in the number of stories.

6.4. The distribution of Maximum Interstory Drift Ratio (MIDR) along the height

The distribution of $MIDR$ along the height of the structure is plotted for some models under Northridge record in 3 various intensity levels ($S_a(T_1, 5\%) = 0.4$ g; 1.0 g; 1.8 g) (Figure 10). It can be seen that the distribution of the $MIDR$ along the height is not uniform. Furthermore, the inelastic behavior is found to be concentrated mainly on the first level and this pattern is maintained with the increase in intensity level. This may happen due to inelastic behavior of the

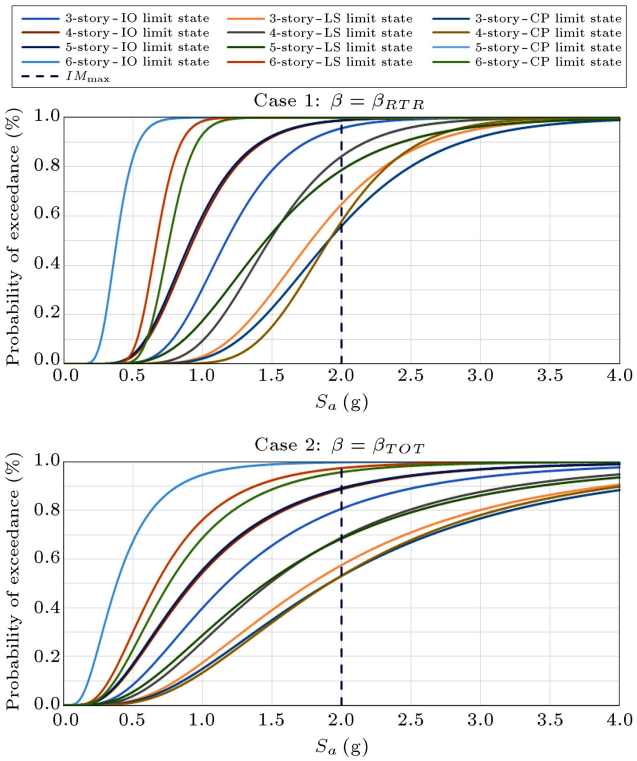

Figure 9. Fragility curves for 4 sets of models (based on the number of stories).

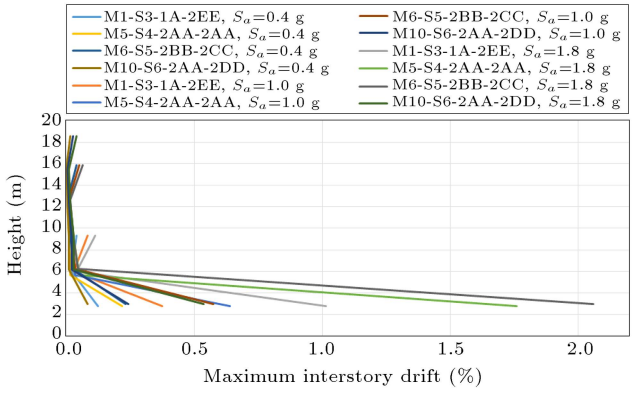

Figure 10. Distribution of the *MIDR* along the height of the structure under Northridge earthquake in 3 various intensity levels ($S_a(T_1, 5\%) = 0.4$ g, 1.0 g, 1.8 g).

braces and the limited redistribution of internal forces in a story in the inelastic range of response.

7. Summary and concluding remarks

In this study, 10 existing residential steel structures with 3 to 6 stories in Qazvin designed during 2010 to 2015 with concentrically braced frames as the seismic force-resisting system in 2 directions were modeled three-dimensionally in OpenSees [18]. Codes used to design the buildings under study included the *Iranian code No. 6 for design loads for buildings* [15], the *Iranian Code No. 2800 for Seismic Restraint Design of Buildings (third edition)* [1], and *the Iranian code No. 10 for Design and Construction of Steel Structures* [16]. From the results obtained, it was concluded that:

- There was a large discrepancy between *IDA* curves obtained using various ground motion records such that some records led to GI in lower intensity levels (e.g. $S_a(T_1, 5\%)$ lower than 1.0 g), while there were some others which did not cause collapse even at $S_a(T_1, 5\%)$ equal to 2.0 g;
- The *IDA* curves were found to have wavy behaviors. The dynamic properties associated with the stiffer braced frames were generally more dramatically changed after the buckling of their braces. The development of scattered points in *IDA* curve was much more likely in such frames due to sensitivity of the interstory drifts to the brace buckling. Furthermore, limitations in alternative loading paths after brace buckling and inelastic behavior concentration on one story along the structure height could lead to wavier form of *IDA* curves. This could be a reasonable explanation for the wavy form of the *IDA* curves for steel structures with braced frames;
- As it could also be predicted by Eq. (2), the fragility curves obtained considering the total uncertainty index β_{TOT}, exhibited lower values of probability of exceeding a limit state at a specific *IM* value than those obtained considering only β_{RTR}. This was due to increase in uncertainties and consequently, in the value of β in the fragility function, which confirmed that record to record variability is the main source of uncertainty in the probabilistic evaluation of the structures;
- The fragility curve was generally pulled back to lower intensity levels as the number of stories increased, indicating that seismic vulnerability generally increased with the rise in the number of stories;
- The distribution of the *MIDR* along the height of the multi-story buildings, which is an important measure of the structural and nonstructural damages to the structure under various intensity levels, was not found to be uniform. This might be due to the loss of compression strength of the brace during several consecutive compression loading cycles after the brace buckling, which in turn led to the reduction in the shear strength of the story and consequently, a significant amount of drift along with the formation of the story mechanism;
- The inelastic behavior was found to be concentrated mainly on the first level and this pattern was maintained with the increase in the intensity level. This might happen due to inelastic behavior of the braces and the limited redistribution of internal forces in a story in the inelastic range of the response.

Acknowledgements

This research was partially supported by the Civil Engineering Department and the Research and Technology Deputy of Sharif University of Technology. The authors also acknowledge the support of *Qazvin Statistics and IT Organization and Qazvin Construction Engineering Organization* for allowing access to the database available for existing buildings in Qazvin and providing us with the required modeling files.

Nomenclature

$S_a(T_1, 5\%)$	Spectral acceleration at fundamental period of the structure with 5% viscous damping
β_{RTR}	Uncertainty index due to record to record variability
β_{DR}	Uncertainty index for quality rating of design requirements
β_{TD}	Uncertainty index for quality rating of test data
β_{MDL}	Uncertainty index for quality rating of index archetype models
β_{TOT}	Total uncertainty index
n	Number of stories
$nbXZ$	Number of braced frames in global X-Z direction
$nbYZ$	Number of braced frames in global Y-Z direction
$IM_{\max}$	The uppermost level of intensity measure in performing truncated IDA
$\Phi()$	The standard normal CDF
$\phi()$	The standard normal PDF
θ	The median of the fragility function
β	The standard deviation of $\ln IM$
IM_i	IM values at collapse for the m ground motions that were observed to cause collapse

Abbreviations

PGA	Peak ground acceleration
DI	Damage index
IM	Intensity measure
IDA	Incremental dynamic analysis
CDF	Cumulative distribution function
PDF	Probability distribution function
EDP	Engineering demand parameter
GMP	Ground motion profile
$conf$	Bracing configuration type
GI	Global instability
PL	Performance level
IO	Immediate Occupancy
LS	Life Safety
CP	Collapse Prevention

References

1. BHRC "Iranian code of practice for seismic resistant design of buildings: Standard no. 2800. 3rd ed", Building and Housing Research Center (2005).
2. Erberik, M.A. and Elnashai, A.S., *Seismic Vulnerability of Flat-Slab Structures*, Mid-America Earthquake Center CD Release 03-06 (2003).
3. Kumar, S.A., Rajaram, C., Mishra, S., Kumar, R.P., and Karnath, A. "Rapid visual screening of different housing typologies in Himachal Pradesh, India", *Natural Hazards*, **85**(3), pp. 1851-1875 (2017).
4. Del Gaudio, C., De Martino, G., Di Ludovico, M., Manfredi, G., Prota, A., Ricci, P., and Verderame, G.M. "Empirical fragility curves from damage data on RC buildings after the 2009 L'Aquila earthquake", *Bulletin of Earthquake Engineering*, **15**(4), pp. 1425-1450 (2017).
5. Toma-Danila, D. and Armaş, I. "Insights into the possible seismic damage of residential buildings in Bucharest, Romania, at neighborhood resolution", *Bulletin of Earthquake Engineering*, **15**(3), pp. 1161-1184 (2017).
6. Tavakoli, B. and Tavakoli, A. "Estimating the vulnerability and loss functions of residential buildings", *Natural Hazards*, **7**(2), pp. 155-171 (1993).
7. JICA, C. "The study on seismic microzoning of the greater Tehran area in the Islamic Republic of Iran", Final Report to the Government of the Islamic Republic of Iran, Tokyo, Japan (2000).
8. Mostafaei, H. and Kabeyasawa, T. "Investigation and analysis of damage to buildings during the 2003 Bam earthquake", *Bulletin of Earthquake Research Institute, University of Tokyo*, **79**, pp. 107-132 (2004).
9. Bakhshi, A. and Karimi, K. "Performance evaluation of masonry buildings using a probabilistic approach", *Scientia Iranica*, **15**(3), pp. 295-307 (2008).
10. Jalalian, M. "Deriving of empirical vulnerability functions for Iran", M.Sc. Thesis, Department of Civil and Environmental Engineering, Sharif University of Technology, Tehran (2006).
11. Kazemi, H., Ghafory-Ashtiany, M., and Azarbakht, A. "Effect of epsilon-based record selection on fragility curves of typical irregular steel frames with concrete shear walls in Mashhad city", *International Journal of Advanced Structural Engineering*, **5**(1), p. 23 (2013).
12. Sadeghi, M., Ghafory-Ashtiany, M., and Pakdel-Lahiji, N. "Developing seismic vulnerability curves for typical Iranian buildings", *Proceedings of the Institution of Mechanical Engineers, Part O: Journal of Risk and Reliability*, **229**(6), pp. 627-640 (2015).

13. Kazemi, H., Ghafory-Ashtiany, M., and Azarbakht, A. "Development of fragility curves by incorporating new spectral shape indicators and a weighted damage index: case study of steel braced frames in the city of Mashhad, Iran", *Earthquake Engineering and Engineering Vibration*, **16**(2), pp. 383-395 (2017).

14. Izanloo, F. and Yahyaabadi, A. "Determination of structural fragility curves of various building types for seismic vulnerability assessment in the Sarpol-e Zahab City", *Journal of Seismology and Earthquake Engineering*, **20**(3), pp. 93-107 (2019).

15. MHUD, *Iranian National Building Code, Part 6, Design Loads for Buildings*, Ministry of Housing and Urban Development, Tehran, Iran (2009).

16. MHUD, *Iranian National Building Code, Part 10, Steel Structure Design*, Ministry of Housing and Urban Development, Tehran, Iran (2009).

17. TABS, *Extended Three Dimensional Analysis of Building Systems*, Computers and Structures, Inc (2011).

18. McKenna, F. "OpenSees: a framework for earthquake engineering simulation", *Computing in Science & Engineering*, **13**(4), pp. 58-66 (2011).

19. Uriz, P. and Mahin, S.A. "Toward earthquake-resistant design of concentrically braced steel-frame structures", PEER rep no. 2008/08. Pacific Earthquake Engineering Research Center, College of Engineering, Univ. of California, Berkeley (2008).

20. Soltanieh, H. "Development of fragility curves for a number of existing buildings in Qazvin", M.Sc. Thesis, Department of Civil and Environmental Engineering, Sharif University of Technology, Tehran (2016).

21. Kinali, K. and Ellingwood, B.R. "Seismic fragility assessment of steel frames for consequence based engineering: A case study for Memphis, TN", *Engineering Structures*, **29**(6), pp. 1115-1127 (2007).

22. Bermúdez, C.A., Barbat, A.H., Pujades, L.G., and González-Drigo, J.R. "Seismic vulnerability and fragility of steel buildings", In *Proceedings of the 14th World Conference on Earthquake Engineering* (2008).

23. Kazantzi, A.K., Righiniotis, T.D., and Chryssanthopoulos, M.K. "The effect of joint ductility on the seismic fragility of a regular moment resisting steel frame designed to EC8 provisions", *Journal of Constructional Steel Research*, **64**(9), pp. 987-996 (2008).

24. Li, Q. and Ellingwood, B.R. "Damage inspection and vulnerability analysis of existing buildings with steel moment-resisting frames", *Engineering Structures*, **30**(2), pp. 338-351 (2008).

25. Ellingwood, B.R. and Kinali, K. "Quantifying and communicating uncertainty in seismic risk assessment", *Structural Safety*, **31**(2), pp. 179-187 (2009).

26. Majd, M., Hosseini, M., and MoeinAmini, A. "Developing fragility curves for steel building with X-bracing by nonlinear time history analyses", In *15th World Conference Earthquake Engineering*, Lisboa (2012).

27. Akbari, R., Aboutalebi, M.H., and Maheri, M.R. "Seismic fragility assessment of steel X-braced and chevron-braced RC frames", *Asian Journal of Civil Engineering (Bhrc)*, **16**(1), pp. 13-27 (2015).

28. Kiani, A., Mansouri, B., and Moghadam, A.S. "Fragility curves for typical steel frames with semi-rigid saddle connections", *Journal of Constructional Steel Research*, **118**, pp. 231-242 (2016).

29. Banihashemi, M.R., Mirzagoltabar, A.R., and Tavakoli, H.R. "Reliability and fragility curve assessment of steel concentrically braced frames", *European Journal of Environmental and Civil Engineering*, **20**(7), pp. 748-770 (2016).

30. Li, G., Dong, Z.Q., Li, H.N., and Yang, Y. B. "Seismic collapse analysis of concentrically-braced frames by the ida method", *Advanced Steel Construction*, **13**(3), pp. 273-292 (2017).

31. Choi, K.S., Park, J.G., and Kim, H.J. "Numerical investigation on design requirements for steel ordinary braced frames", *Engineering Structures*, **137**, pp. 296-309 (2017).

32. Díaz, S.A., Pujades, L.G., Barbat, A.H., Hidalgo-Leiva, D.A., and Vargas-Alzate, Y.F. "Capacity, damage and fragility models for steel buildings: a probabilistic approach", *Bulletin of Earthquake Engineering*, **16**(3), pp. 1209-1243 (2018).

33. Fattahi, F. and Gholizadeh, S. "Seismic fragility assessment of optimally designed steel moment frames", *Engineering Structures*, **179**, pp. 37-51 (2019).

34. Sinha, R. and Shiradhonkar, S.R. "Seismic damage index for classification of structural damage-closing the loop", In *the 15th World Conference on Earthquake Engineering* (2012).

35. Bani Asadi, A. "Application of damage indices in seismic analysis of concrete frames using endurance time method", M.Sc. Thesis, Department of Civil and Environmental Engineering, Sharif University of Technology, Tehran (2012).

36. Pitilakis, K., Argyroudis, S., Kakderi, K., Argyroudis, A., Crowley, H., and Taucer, F., *Systemic Seismic Vulnerability and Risk Analysis for Buildings, Lifeline Networks and Infrastructures Safety Gain*, Publications Office of the European Union (2013).

37. Mackie, K. and Stojadinović, B., *Seismic Demands for Performance-Based Design of Bridges*, Pacific Earthquake Engineering Research Center (2003).

38. Fathieh, A. "Nonlinear dynamic analysis of modular steel buildings in two and three dimensions", Doctoral dissertation, Department of Civil and Environmental Engineering, University of Toronto, Toronto (2013).

39. FEMA, P695, *Quantification of Building Seismic Performance Factors*, prepared by the Applied Technology Council, Redwood City, California for the Federal Emergency Management Agency, Washington, DC (2009).

40. http://peer.berkeley.edu/products/strong_ground_motion_db.html

41. Lee, T.H. and Mosalam, K.M. "Seismic demand sensitivity of reinforced concrete shear-wall building using FOSM method", *Earthquake Engineering and Structural Dynamics*, **34**(14), pp. 1719-1736 (2005).

42. Koutromanos, I. and Shing, P.S. "Example application of the FEMA P695 (ATC-63) methodology for the collapse performance evaluation of reinforced masonry shear wall structures", In *Proc., 9th US National and 10th Canadian Conf. on Earthquake Engineering* (2010).

43. Donovan, L.T. and Memari, A.M. "Determination of seismic performance factors for structural insulated panel shear walls based on FEMA P695 methodology", *PHRC Research Series Rep*, **110** (2011).

44. Pragalath, D.H. and Sarkar, R.D.P. "Reliability evaluation of RC frame by two major fragility analysis methods", *Asian Journal of Civil Engineering (BHRC)*, **16**(1), pp. 47-66 (2015).

45. Siyam, M. "Seismic performance assessment of ductile reinforced concrete block structural walls", Doctoral Dissertation, Department of Civil and Environmental Engineering, McMaster University, Ontario (2016).

46. Hsiao, P.C., Lehman, D.E., and Roeder, C.W. "A model to simulate special concentrically braced frames beyond brace fracture", *Earthquake Engineering & Structural Dynamics*, **42**(2), pp. 183-200 (2013).

47. Mazzoni, S., McKenna, F., Scott, M., and Fenves, G., *Open System for Earthquake Engineering Simulation (OpenSEES) User Command-Language Manual*, Pacific Earthquake Engineering Research Center., University of California, Berkeley (2006).

48. Vamvatsikos, D. "Seismic performance, capacity and reliability of structures as seen through incremental dynamic analysis", Doctoral Dissertation, Department of Civil and Environmental Engineering, Stanford University, Stanford, Palo-Alto, CA (2002).

49. Baker, J.W. "Efficient analytical fragility function fitting using dynamic structural analysis", *Earthquake Spectra*, **31**(1), pp. 579-599 (2015).

50. FEMA, *Commentary for the Seismic Rehabilitation of Buildings*, FEMA-356, Federal Emergency Management Agency, Washington, DC (2000).

51. MATLAB, *The Language of Technical Programming*, the Mathworks Inc (2010).

52. Vamvatsikos, D. and Cornell, C.A. "Direct estimation of seismic demand and capacity of multidegree-of-freedom systems through incremental dynamic analysis of single degree of freedom approximation", *Journal of Structural Engineering*, **131**(4), pp. 589-599 (2005).

Biographies

Ali Bakhshi earned his BSc and MSc degrees in Civil and Structural Engineering from Sharif University of Technology (SUT) and Shiraz University in 1988 and 1990, respectively. In 1998, he received his PhD from Hiroshima University, Japan, where he became a faculty member in the same year. In 2000, he moved to SUT, where he is currently an Associate Professor. He was actively involved in design and installation of the shaking table facility and since then, Dr. Bakhshi has been contributing to many experimental testing types of research. He is the director of earthquake simulation national LAB and the head of the Earthquake Engineering Research Center at Sharif University of Technology at present. Dr. Bakhshi's main interests include experimental and analytical research on earthquake engineering, specifically structural control, seismic performance of adobe structures, seismic hazard and risk analyses, and random vibrations. He has published more than 60 papers in international journals and conferences.

Hamideh Soltanieh received her BSc and MSc degrees in Civil Engineering from the Department of Civil Engineering at Imam Khomeini International University, Qazvin, Iran, and Sharif University of Technology, Tehran, Iran, respectively. She graduated in January 2016. Her field of research includes seismic hazard analysis, *IDA*, steel structures, and fragility curves.